



# Excitation Frequency Effect on Breast Cancer Cell Death by Atmospheric Pressure Cold Plasma

V. Chaturvedi Misra<sup>1,3</sup> · Ganesh Pai B<sup>2,3</sup> · N. Tiwari<sup>1</sup> · B. S. Patro<sup>2,3</sup> · S. Ghorui<sup>1,3</sup>

Received: 8 July 2022 / Accepted: 11 January 2023 / Published online: 29 January 2023

© The Author(s), under exclusive licence to Springer Science+Business Media, LLC, part of Springer Nature 2023

## Abstract

The tuning capacity of a novel excitation frequency controlled cold atmospheric pressure plasma jet in terms of reactive species density and its biological effect i.e., cell proliferation with changes in the excitation frequency was examined. The various reactive species produced were identified using optical emission spectroscopy. The physicochemical properties of the PTW (Plasma Treated Water) generated by the source were found to be almost linearly related with the time of treatment. For the presence of reactive species ( $\text{H}_2\text{O}_2$ ,  $\text{NO}_3^-$  and  $\text{NO}_2^-$ ), a comparison of plasma-treated water and cell culture medium at 11 kHz has been established. It has been observed that the variation in excitation frequency and treatment duration have important impact on cancer cell viability. In this regard, measuring the induced reactive species confirmed the strongest effect with CAP generated at 11 kHz frequency. Additionally, the 11 kHz frequency CAP produced the best biological outcome, among the different frequencies tested i.e., 11, 14, 22 and 26 kHz, as assessed by the reduction in proliferation of two different breast cancer cells (MCF-7 and MDA-MB-231). Further, the mechanistic aspects of CAP generated with 11 kHz frequency in inducing breast cancer cell death were investigated. The cancer cell death was rescued by co-treatment with N-acetyl cysteine, which indicated that the cell death effected by CAP is through the generation of reactive oxygen species. It has been shown that 11 kHz frequency CAP treatment induces excessive DNA damage and a prominent G1 phase cell cycle arrest and consequently cell death by apoptosis.

**Keywords** EFCAP · Optical emission spectroscopy · kHz discharge · Breast cancer cells · Reactive oxygen species

---

✉ V. Chaturvedi Misra  
vandanachaturvedi15@gmail.com; vandana@barc.gov.in

<sup>1</sup> Laser & Plasma Technology Division, Bhabha Atomic Research Centre, Trombay, Mumbai 400085, India

<sup>2</sup> Bio-Organic Division, Bhabha Atomic Research Centre, Trombay, Mumbai 400085, India

<sup>3</sup> Homi Bhabha National Institute, Anushaktinagar, Mumbai 400095, India

## Introduction

Research on low temperature cold atmospheric pressure plasma (CAP) jets has been extensively growing due to its applications in a variety of fields. So far, CAPs have been studied for material processing [1, 2], surface disinfection [3], dentistry [4, 5], wastewater purification [6], antimicrobial applications [7, 8] and cancer treatment [9, 10]. Presence of various reactive species such as reactive oxygen species (ROS:  $O_2^-$  and  $\bullet OH$ ) and reactive nitrogen species ( $\bullet NO$  and  $\bullet NO_2$ ) are believed to make the plasma jets useful for these applications [11, 12]. Also, when such species containing jets are produced over a medium, the reactive species formed in the glow region above the medium get transferred into the medium and activate it. This treated medium is known as plasma treated medium and has been reported to be extremely useful for cancer treatment [13–15].

According to the World Health Organization, approximately 10 million people died due to cancer in 2020 [16]. Out of all these deaths around 70% deaths occur in low- and middle-income countries. In 2020 alone, around 19 million new cancer cases were reported globally [17] and around 11.7% were breast cancer cases. Globally, breast cancer is the most commonly diagnosed type of cancer, standing fifth in cancer related deaths (6.9%) [18]. Despite the availability of multiple efficient chemotherapies, several side effects [19] associated with these drugs necessitate the exploration of novel therapeutic modalities and combinatorial approaches. Additionally, the cancer cells invariably develop resistance to these chemotherapeutics resulting in treatment failure [20, 21]. Intriguingly, certain studies have found that CAP can restore the sensitivity of chemo-resistant cancer cells to specific drugs [22–24]. Hence, effective CAP based therapies and further combinatorial approaches of chemotherapeutics with CAP are the need of the hour.

CAP exposure selectively causes death in tumour cells and having less or no effect on normal cells [25, 26]. Wang et al. [25] could establish the selectivity with human metastatic breast cancer cells and bone marrow derived human mesenchymal stem cells (MSCs) at an output voltage of 3.68 kV for treatment duration of more than 60 s and distance of 3 cm from source to plate bottom. The selectivity could not be established for less than 60 s treatment. Since, the cancer cells proliferate much faster than normal cells, it was concluded that CAP could selectively target cancer cells by interfering with the mitotic cell cycle at the same dose. Similarly, Preston et al. [26] showed that it is possible to tune the settings of plasma to specifically target the cancer cells (JHU-O28 and SCC25) at 8 kV, helium flow rate of 10 l/min at a distance of 3 cm from source to cells for 30 s of treatment while leaving the normal tissue (JHU-022 and JHU-029) unharmed. The selectivity shown with CAP treatment may be due to higher levels of antioxidants in normal cells *vis-à-vis* cancer cells that may prevent ROS concentrations to reach the threshold to induce apoptosis at the same challenging dose. However, higher doses may also harm the normal cells [27].

Different geometries of CAPs have been reported in literature like pin to plane discharge [28], dielectric barrier discharge [29], and coaxial configuration [30]. Also, many studies have used a fixed frequency source of 13.56 MHz [31, 32] and have paid attention mostly on the application itself. Though it is important to understand the effect of plasma discharge on various applications, the effect of change in the driving frequency should not be ignored. In view of the above, a non-dielectric excitation frequency

controlled cold atmospheric plasma (EFCAP) has been developed with a coaxial configuration to study the effect of changing driving frequencies on reactive species density and study the effect of these on human breast cancer cells.

To the best of authors' knowledge, this is the first study of EFCAP showing potential for the treatment of breast cancers. A thorough research with variable driving frequencies have established the fact that a change in the frequency has a capability to tune the reactive species [33, 34] and the present study shows the effect of these frequencies on the breast cancer cells. The study employs a recently reported [33, 34] continuously tunable excitation frequency controlled cold atmospheric pressure plasma (CAP) device. EFCAP emphasizes the 'excitation frequency' control feature of the discharge. Fast switching induced high voltage in the secondary coil of a transformer results in breakdown in the electrode gap in the device initiating the discharge. Once plasma fills the gap in the device, an LCR (L- Inductor, C-Capacitor, R-Resistor) tank circuit forms with the secondary coil in the loop. The discharge sustains via damped oscillation of the field inside the plasma till the next external excitation pulse comes and initiates a fresh discharge [33]. The net consumed power in the process is of the order of few watts.

Although frequencies over a broad range have been investigated, the deployed frequency mostly remained fixed for a particular study. While it is undoubtedly important, the effect of driving frequency on the produced plasma and associated applications are not explored enough. The present study focuses on this specific aspect. The plasma jet generated is characterized for its physicochemical parameters in plasma treated water such as hydrogen ion concentration (pH), electrical conductivity (EC), nitrate ( $\text{NO}_3^-$ ), nitrite ( $\text{NO}_2^-$ ) and hydrogen peroxide ( $\text{H}_2\text{O}_2$ ). The effect of excitation frequency and the time of treatment on two different human breast cancer cells (MCF-7) and (MDA-MB-231) are evaluated. The effect of ROS and the mechanism of CAP induced cell death is also investigated.

## Materials and Methods

### Excitation Frequency Controlled Atmospheric Pressure Plasma Jet Source

EFCAP used in the present study is shown in Fig. 1. The used operating parameters are listed in Table 1. Gas flow rates mentioned in Standard Litres Per Minute (SLPM) were

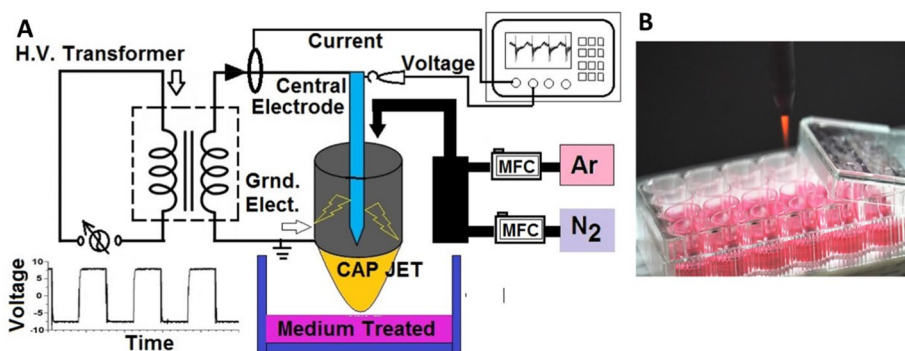


**Fig. 1** A Schematic of the used EFCAP device and its operation [33]; B Image of the plasma treatment of cancer cells

**Table 1** Plasma Operating Parameters

Parameters	Values
Argon flow rate (SLPM)	18
N <sub>2</sub> flow rate (SLPM)	0.8
Treatment distance from nozzle exit to well top (mm)	15
Excitation frequencies (kHz)	11, 14, 22, 26
Supply voltage (V)	18.5

measured using mass flow controllers. Voltage and current were measured using probes supplied by Tektronix P6015A voltage probe and P6021 current probe. The V–I signals were sampled using a Hameg (HMO3524) oscilloscope. The source design confined the discharge in the nozzle section. The discharge zone of 2 mm radius was formed between the central tungsten electrode (diameter 2 mm) and the surrounding SS 304 electrode (inner diameter 6 mm). The plasma jet of 15 mm length was formed at 11 kHz.

Some of the distinctive features of the device include simple design, discharge without dielectric barrier, ability to operate with argon (replacing expensive helium), and control of discharge characteristics by tuning of external driving frequency. Dissipated power, discharge frequency, electron temperature, gas temperature, and species density are the important parameters that can be directly controlled through external frequency tuning.

## Characterization Studies

The treatment of 20 ml water (High purity water, Merck, Germany) at different frequencies and time of treatment was studied for its physicochemical parameters. Table 2 lists the equipment used for the characterization studies of Plasma Treated Water (PTW). The pH meter was calibrated at two points using standard buffer solutions of pH 7.01 (Hanna Instruments) and pH 4.01 (Hanna Instruments). The EC tester was calibrated with a calibration solution of standard conductivity of 1413  $\mu\text{S}/\text{cm}$ . (Rakiro Biotech). Quantofix strips (Macherey Nagel) were used to determine H<sub>2</sub>O<sub>2</sub>, NO<sub>2</sub><sup>-</sup> and NO<sub>3</sub><sup>-</sup> in solutions using a test strip reflectometer (Quantofix relax- Macherey-Nagel, Germany). The system auto calibrated each time the system was switched on for the chosen range of the test type. The test strip was placed on a measuring slide with inbuilt reference pad. A light source illuminated the test pad and a detection unit then measured the intensity of the reflected light at three different wavelengths, from which the value was calculated. The reaction time for every test is pre-programmed and the strip was placed on the strip slide of the reader immediately after immersing into the sample. The reader measured with an error of  $\pm 20\%$ .

20 ml water (initial EC =  $2 \pm 1 \mu\text{S}/\text{cm}$ , pH  $6.7 \pm 0.5$ ) was taken in a glass beaker and treated with plasma jet at 15 mm from the nozzle exit for 4, 8, 12, 16 and 20 min. Initial concentration in untreated water for NO<sub>3</sub><sup>-</sup>, NO<sub>2</sub><sup>-</sup> and H<sub>2</sub>O<sub>2</sub> was found to be below 10 ppm ( $\pm 20\%$ ), 0.5 ppm ( $\pm 20\%$ ) and 0.5 ppm ( $\pm 20\%$ ), respectively. The EC, pH, NO<sub>3</sub><sup>-</sup>, NO<sub>2</sub><sup>-</sup> and H<sub>2</sub>O<sub>2</sub> were measured first for 4 min treatment. The electrode was inserted and a stable EC and pH was reached after 3 s and 10 s, respectively. NO<sub>3</sub><sup>-</sup>, NO<sub>2</sub><sup>-</sup> and H<sub>2</sub>O<sub>2</sub> were measured using the test strips to determine H<sub>2</sub>O<sub>2</sub>, NO<sub>2</sub><sup>-</sup> and NO<sub>3</sub><sup>-</sup> in solutions quickly. One strip

**Table 2** Equipment used to measure physicochemical parameters of PTW

Parameter	Equipment	Range (precision)
EC	Aquasol EC/TDS meter (AM-P-EC, E213835, India)	0–9,990 $\mu\text{S}/\text{cm}$ (1 $\mu\text{S}/\text{cm}$ )
pH	Hanna pHepTester (HI98107P, USA)	0–14 (0.1)
$\text{NO}_3^-$	Quantofix Nitrate strips* (Macherey-Nagel, Germany)	10–500 mg/L (1 mg/L)
$\text{H}_2\text{O}_2$	Quantofix peroxide-25*, peroxide-100* strips (Macherey-Nagel, Germany)	0.5–25 mg/L (1 mg/L) 1–100 mg/L (1 mg/L)
$\text{NO}_2^-$	Quantofix Nitrite strips*	1–80 mg/L (1 mg/L)

\*The test strip colour was read using Quantofix Relax reflectometer (Machery Nagel, Germany- QR 0323)

was dipped in plasma treated water and placed on test strip holder of the Quantofix relax reflectometer. To maintain the purity of the water; the water once evaluated was discarded and then fresh 20 ml was taken for analysis of 8 min treatment and so on. The testing parameters other than the treatment duration were kept identical during all these experiments at a fixed frequency. The frequency was then varied, and the next sets of experiments were performed.

Each test was carried out three times; graphs for pH and EC show the mean value with the standard deviation as an error bar. The error bar for  $\text{NO}_3^-$ ,  $\text{NO}_2^-$  and  $\text{H}_2\text{O}_2$  shows the error of  $\pm 20\%$  as given by the test strip reader.

## Optical Emission Spectroscopy (OES)

A high-resolution spectrometer [Shamrock 303i, Andor, UK] having maximum spectral resolution of 0.07 nm was used to identify species and record spectral features of the emitted lines in the range 200–900 nm. The optical fibre probe was installed 2 mm away from the plasma jet nozzle.

## Biological Studies

### Materials

Crystal violet (CV), propidium iodide (PI), N-acetyl cysteine (NAC), Hoechst 33258, Triton X-100, Tween-20, Antibodies-  $\gamma\text{-H2AX}$  (#H5912), 53BP1 (#05–636) were purchased from Sigma-Aldrich (St. Louis, MO, USA). 0.05% Trypsin–EDTA (1X) solution and Fetal Bovine Serum (FBS) were procured from Gibco-Thermo Fischer Scientific (Waltham, MA, USA), Dulbecco's Modified Eagle's medium (DMEM) (#AL007G), Antibiotic and antimycotic solution (#A002, 100X liquid with penicillin, streptomycin and amphotericin B) were procured from HiMedia Laboratories (Mumbai, India). Unless and otherwise specified, all the other fine chemicals were procured from Sigma-Aldrich (St. Louis, MO, USA).

## Methods

**Cold-Atmospheric Plasma Treatment** The treatment is as per the schematic given in the respective figures. The distance measured is between the uppermost surface of the plate/micro-centrifuge tube to the tip of the nozzle of CAP discharge. The details regarding the frequency of CAP treatment and the time duration of exposure of CAP in each experiment has been described in the legends section or the protocol part of the respective figures. Table 3 includes the details of the medium treated in each assay.

**Cell Culture and Cell Lines** Breast invasive ductal adenocarcinoma cells, MCF-7, and triple negative breast cancer cells and MDA-MB-231 cell lines are procured from National Centre for Cell Sciences, India. The cell lines are maintained in DMEM with 10% FBS and 1x antibiotic and antimycotic solution in an incubator (95% relative humidity; 5% CO<sub>2</sub>; 37 °C).

**Proliferation Assay** Cells ( $5 \times 10^4$ ) were seeded in a 24-well plate. After overnight incubation, CAP treatment is given. Post 48 h, the spent media was discarded, washed twice with phosphate buffered saline (PBS) and fixed with methanol. Further, the adherent live cells were stained with the crystal violet solution (0.25 % CV in 20 % methanol solution, v/v in distilled water). After incubation for 15 min, the wells were washed thoroughly and then lysed in a lysing solution (0.1 M sodium citrate solution) in 50 % ethanol (v/v in distilled water; pH 4.2 adjusted with HCl) for 15 min. 100  $\mu$ L from each well is then transferred into a 96 well plate and is read in triplicates (technical replicates). Absorbance is measured at 590 nm wavelength in a microplate reader (BMG Labtech, Ortenberg, Germany).

**Sub-G1 Population and Cell Cycle Analyses by Flow Cytometry** Flow cytometry analyses for sub-G1 population and cell cycle were carried out as per previously reported methods on flow cytometer (Partec/Sysmex Cyflow Space, Germany) [35]. Briefly, sub-confluent growing breast cancer cells were trypsinized and cell suspension of  $1.5 \times 10^5$  cells per mL was prepared in a 1.5 mL microcentrifuge tube. Thereafter, this cell suspension was treated with CAP and seeded in a 12-well plate. 24 h later, samples were trypsinized and processed for cell cycle analysis after staining with propidium iodide (PI) in the hypotonic sodium citrate buffer solution with 0.1 % Triton X-100.

Similarly, the cells were processed for subG1 population analysis and analyzed 48 h after 11 kHz frequency CAP treatment for 75, 150 and 300 s as indicated in the respective figure legends.

**Clonogenic Assay** Cell suspensions ( $1.5 \times 10^5$  cells per mL) were treated with CAP as indicated in the respective figure legends and the cell viability and clonogenic assays were performed as reported earlier [35].

**Light Microscopy** Cell suspension of breast cancer cells,  $1.5 \times 10^5$  cells per mL, were treated with cold atmospheric plasma for the mentioned time duration and were plated onto a 6 well plate. Cells were observed under a microscope after 4 h. Leica microscope (Leica Microsystems, Germany) equipped with LAS EZ software was used for image capture.

**Confocal Microscopy** The method for confocal microscopy used is as described earlier with minor modifications [36]. Briefly, after the cell suspensions ( $1.5 \times 10^5$  per tube) were treated with the 11 kHz frequency for 75, 150 or 300 s and they were seeded on glass cover slips in a 6-well plate. After 6 h incubation, the cells were fixed with methanol for 10 min following phosphate-buffered saline solution (PBS) wash. Fixed samples were then permeabilized using PBS containing 0.1% Triton X-100 for 10 min and blocked with bovine serum albumin (BSA; 5% w/v in PBS). 53BP1,  $\gamma$ -H2AX antibodies at 1:5000 dilutions were added in BSA in PBS (2.5% w/v) and incubated overnight at 4 °C. Further, three washes with PBS containing 0.1% Tween-20 (PBST) were given to the samples and incubated with secondary antibody conjugated with Alexa Fluor 488/594 in BSA in PBST (2.5% w/v) for 3 h. These samples were later washed with PBST, mounted on glass slides with 80% glycerol containing Hoechst 33258 (25  $\mu$ M) and the images are captured by LSM 780 laser scanning confocal microscope (Carl Zeiss, Oberkochen, Germany). A minimum of 50 cells are analyzed for each treatment condition in each experiment. Image analysis is performed using Zeiss Zen 2011 software.

**Statistical Analysis** All biological experiments were performed at least three times ( $n = 3$  biological replicates) and their values are indicated as mean  $\pm$  SD. The number of technical replicates, wherever they apply, are mentioned in the legends section of the respective figures. GraphPad Prism 8.0 was used for statistical analysis. Details of the statistical significance test performed are mentioned in the respective legends. A value of  $p < 0.05$  is considered significant.

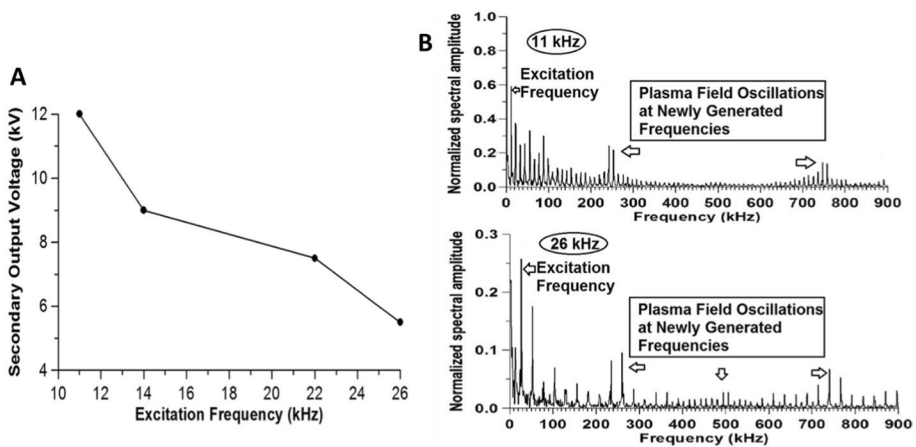


**Fig. 2** **A** Variation of output voltage at the secondary of the transformer as a function of excitation frequency **B** Observed field oscillation inside the plasma over a broad spectral range with dominant peaks at particular frequencies [33]

## Results and Discussion

### EFCAP Power Supply Characteristics

In the device every falling edge of the input square pulse generates a very high voltage pulse across the secondary without fail. However, the pulse height ( $\sim 12$  kV at 11 kHz) across the secondary diminishes with increase in excitation frequency ( $\sim 5.5$  kV at 26 kHz) [See Fig. 2A]. While the use of diode in the secondary helps in achieving high voltage across it, observed decrease in the height of the secondary pulse is expected to occur at higher frequency due to decrease in the effective primary voltage. For a given supply voltage (18.5 V) the enhanced back EMF (Electromotive force) in the primary at higher excitation frequency lowers the effective voltage applied across the primary as per Lenz's law. Higher secondary voltage at lower excitation frequency gives higher ionization, higher reactive species and higher reactive species concentrations as observed in the results of the subsequent sections.

Interestingly, the external excitation at a specific frequency (kHz range) effectively induces a field oscillation in the plasma that encompasses broad spectral range having frequency components even close to MHz order. It is believed that the newly generated frequency components of the oscillation originate through interaction of the external field with the field produced by the plasma species itself [Fig. 2B].

A high-speed camera (Model No PCO 1200hs, 1280 X 1024 pixels CMOS sensor) was employed to grab the fast-changing discharge zone features with the changing excitation frequencies. The end on images were captured of the discharge zone in between the electrodes at 150 cm from the nozzle exit. Importantly, it was the oscillation of the field inside the plasma that eventually enabled it to inherit its ability to offer specific species densities and particular process chemistry. Direct evidence of nonlinear interaction of the oscillating field with the plasma were manifested through complex bunching pattern inside the discharge zone in the form of evolving spiral filaments and local hot spots as observed in Fig. 3.

Evolution of such patterns, frequency of induced oscillations and their dependence on excitation frequency have been reported in detail in [33]. While mentioned features establishing the novelty of the device, some typical patterns observed at different excitation

**Fig. 3** Distinct patterns evolved through plasma-field interaction in the form of spirals and hot spots at various excitation frequencies 11 kHz [33], 14 kHz, 22 kHz and 26 kHz [Drawn circle presents the exit bore of the torch (6 mm diameter)]

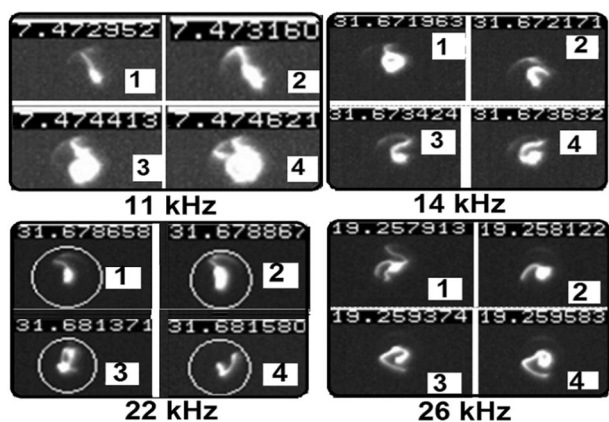




**Table 3** Details of the medium treated in each assay

Assay	Medium used	Volume of the medium	Treatment duration	Incubation duration
Proliferation assay for different frequencies	DMEM with 10% FBS and 1 × antibiotic and antimycotic solution	2 ml	150 s	48 h
Proliferation assay for treatment time at 11 kHz	DMEM with 10% FBS and 1 × antibiotic and antimycotic solution	2 ml	60 s, 120 s, 180 s	48 h
Proliferation assay with NAC for different treatment duration at 11 kHz	DMEM with 10% FBS and 1 × antibiotic and antimycotic solution + NAC	2 ml	50 s, 75 s, 150 s	48 h
Sub G1 assay	DMEM with 10% FBS and 1 × antibiotic and antimycotic solution	2 ml	75 s, 150 s, 300 s	24 h
Clonogenic assay	DMEM with 10% FBS and 1 × antibiotic and antimycotic solution	2 ml	75 s, 150 s, 300 s	8–10 days
Light Microscopy	DMEM with 10% FBS and 1 × antibiotic and antimycotic solution	2 ml	75 s, 150 s, 300 s	4 h
Confocal Microscopy	DMEM with 10% FBS and 1 × antibiotic and antimycotic solution	2 ml	75 s, 150 s, 300 s	24 h

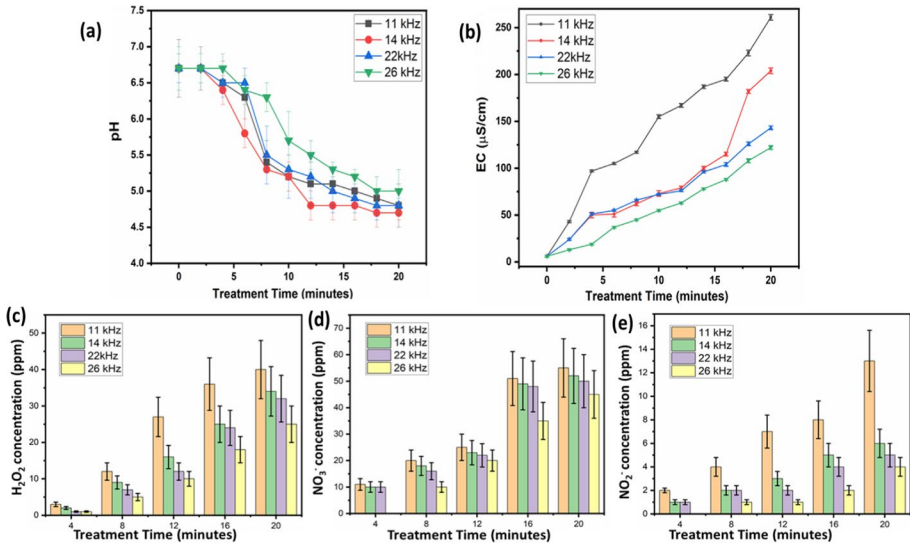


**Fig. 4** Variation of chemical parameters with excitation frequency in plasma treated high purity deionized water (20 ml). **A** pH; **B** EC; **C**  $\text{H}_2\text{O}_2$  concentration **D**  $\text{NO}_3^-$  concentration and **E**  $\text{NO}_2^-$  concentration

frequencies are presented in Fig. 3, for sake of understanding and completeness. It may be noted that the salient features of the patterns change with excitation frequency change. Numeric printed on each image is the time stamp (in seconds) of the instant of grabbing the image using fast camera.

### pH, EC, $\text{NO}_3^-$ , $\text{NO}_2^-$ and $\text{H}_2\text{O}_2$ Concentration

To establish a linear response of the reactive species generation with time and tunability at different frequencies; pH, EC,  $\text{NO}_3^-$ ,  $\text{NO}_2^-$  and  $\text{H}_2\text{O}_2$  concentration were measured of plasma treated water.

pH is a measure of hydrogen potential, which specifies acidity or basicity of an aqueous solution, while EC is a measure of water's ability to conduct electric current. The EC of a solution is mostly determined by the ions present in the solution. Many processes are responsible for the generation of ions and radicals in water when plasma species interact with water molecules, according to the literature [37–40]. Table 3 (Supplementary information) is a list of some of these reactions' pathways. These ions and molecules change the pH and EC of the water after plasma treatment. The decrease in pH (Fig. 4A) and increase in EC (Fig. 4B) with an increase in excitation frequency of the plasma are the results of generation of several acidic chemical species. A higher secondary voltage (~12 kV) at lower excitation frequency of 11 kHz results into higher ionization and higher reactive species concentrations as compared to 26 kHz (~5.5 kV). This feature enables tunability with change in frequency keeping all other input parameters constant. Higher EC and lower pH are observed as treatment time increases since it is expected that more chemical species will form with time.

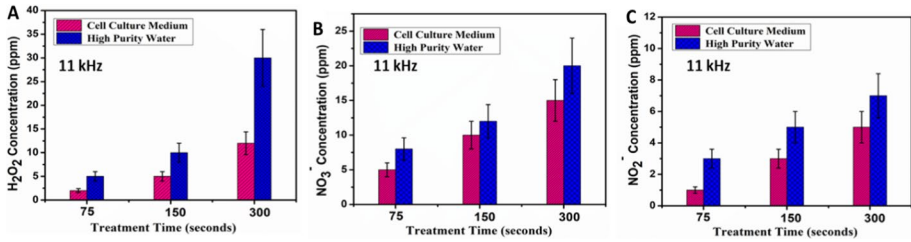


**Fig. 5** Variation of chemical parameters at 11 kHz excitation frequency in plasma treated Cell Culture medium (2 ml) and high purity deionized water (2 ml). **A** H<sub>2</sub>O<sub>2</sub> concentration; **B** NO<sub>3</sub><sup>-</sup> concentration and **C** NO<sub>2</sub><sup>-</sup> concentration. Cell Culture medium consists of DMEM with 10% FBS and 1× antibiotic and antimycotic solution, used to maintain the cancer cell lines during the experiments

It is worthy to mention here that as the frequency is reduced from 26 to 11 kHz; the height of the voltage developed across transformer secondary rises due to reduced back-EMF induced in the primary as per Lenz’s law [33]. But the average primary current rises from 1.7 A to 3.5 A as the excitation frequency reduces to 11 kHz. Further lowering of excitation frequency results in primary current high enough to exceed the maximum current carrying capacity of the used MOSFET switch. Therefore, the minimum safe

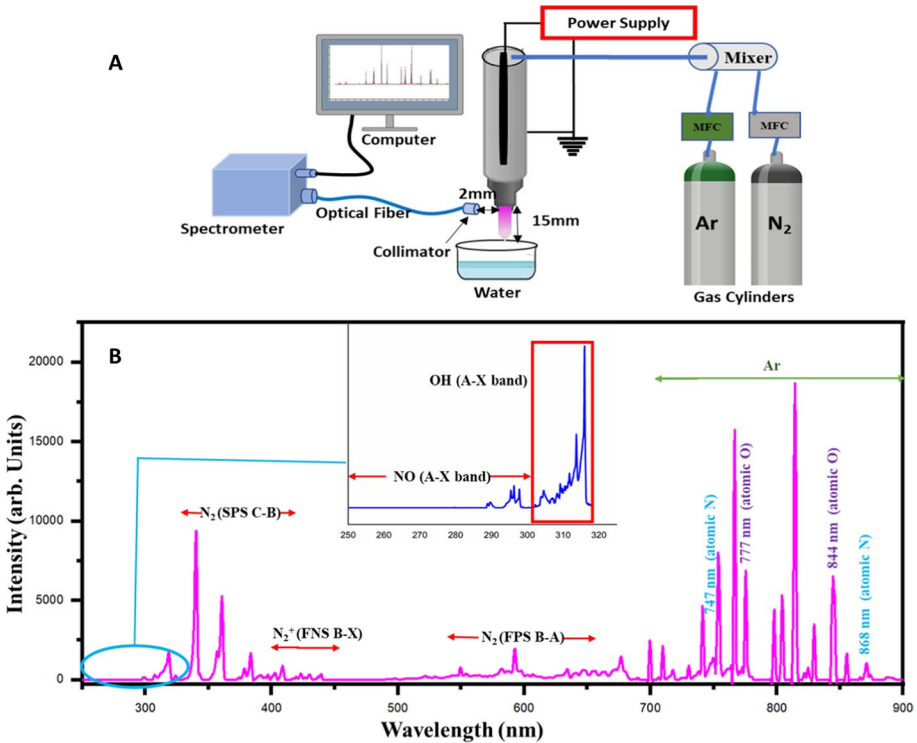


**Fig. 6** Optical emission characteristics of the jet. **A** Experimental set up **B** Spectra recorded at 22 kHz excitation. Different species like OH, NO, atomic oxygen and atomic nitrogen are observed along with argon and N<sub>2</sub> lines

excitation frequency possible with the present design of the power supply is 11 kHz. Also, a higher voltage across the transformer secondary is expected below 11 kHz which may result in higher power deposition into the plasma. Higher power could increase the gas temperature of the plasma jet beyond 50 °C and could make the source unsuitable for bio-medical applications [34]. The gas temperature at different excitation frequencies has been measured and reported elsewhere [34].

A tendency of lower pH value is noted in Fig. 4A as excitation frequency increases from 11 to 14 kHz. Interestingly the pH value increases again as one reaches 26 kHz. For a low frequency discharge between two bare electrodes, both ions and electrons may get enough time to get collected by respective electrodes. However, as frequency increases bulky ions may not get sufficient time for collection before field reversal takes place. Resulting accumulation of positive charges inside the discharge zone causes field enhancement which in turn contributes generation of more radicals through ionization [33]. Naturally pH value goes down in such cases. However, if frequency of the exciting field goes very high, a time comes when even the electrons do not get enough time for complete clearance. In such cases, it is suspected that accumulation of negative electrons inside the discharge zone drastically reduces the field enhancement factor. Observed increase in pH value at excitation frequency of 26 kHz might have occurred from reduced radical generation in such scenario. Observed variation in the electrical conductivity value in Fig. 4B also can be explained in similar way. A number of reactions govern how the reactive species dissolved in the medium interact with the plasma generated species (electrons, photons, radicals, etc.), which in turn affects the ion concentration (pH and EC) in the liquid [41].

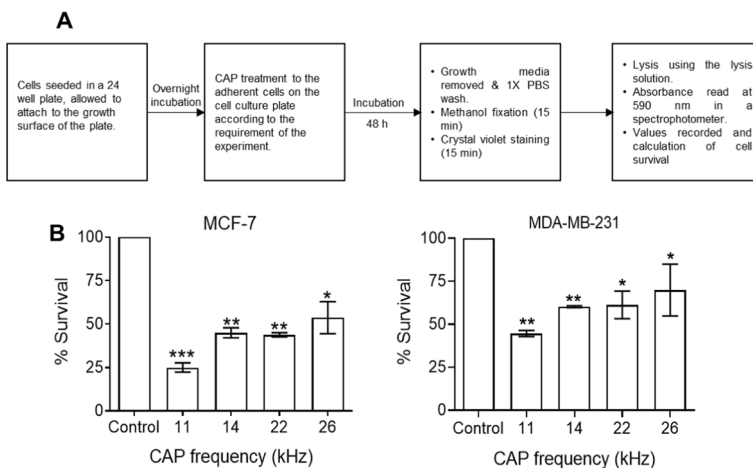


**Fig. 7** Effect of different frequencies of CAP in reducing the proliferation of breast cancer cells. **A** Schematic showing the protocol for the treatment of cancer cells with CAP and further analysis of cell proliferation. **B** MCF-7 cells or MDA-MB-231 cells are treated with different frequencies of CAP for 150 s duration as per the protocol given in Figure A and allowed to grow. 48 h post treatment, proliferation of cells is analysed by staining with crystal violet and solubilizing using the lysis solution and the absorbance of this solution is measured at 590 nm. Quantifications are indicated as percentage survival, control group as 100%. ( $n=3$  biological replicates with at least 3 technical replicates in each experiment). ANOVA (analysis of variance) test was performed and the mean of each group was compared with every other group mean. \* $p < 0.05$  and \*\* $p < 0.01$  compared to respective untreated control group

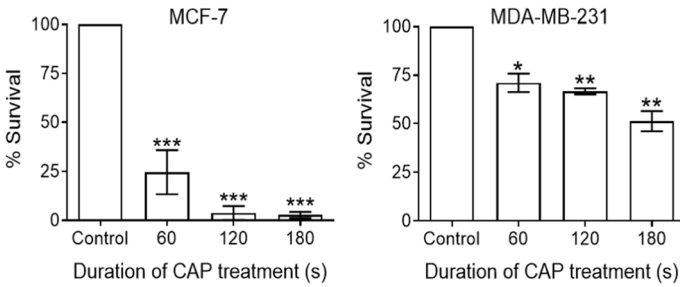


**Fig. 8** CAP reduces proliferation of MCF-7 and MDA-MB-231 breast cancer cell lines at 11 kHz excitation. MCF-7 cells or MDA-MB-231 cells are treated with 11 kHz frequency CAP for the indicated durations as per the protocol given in Fig. 7A and allowed to grow, 48 h post treatment proliferation of cells is analysed. Quantifications are shown. ( $n=3$  biological replicates with at least 3 technical replicates in each experiment). ANOVA test was performed and the mean of each group was compared with every other group mean. \* $p < 0.05$ , \*\* $p < 0.01$  and \*\*\* $p < 0.001$  compared to respective untreated control group

One of the most stable species formed directly by plasma water interaction is hydrogen peroxide.  $H_2O_2$  is thought to be formed mostly through  $\bullet OH$  radical recombination [37]. High-energy electron dissociation of water [37] or metastable argon interaction [38] produce these  $\bullet OH$  radicals.  $NO_3^-$  and  $NO_2^-$  is generated in water when  $\bullet NO_2$  is produced by plasma-air interaction [42]. Nitrate ion can also be formed by the reaction of nitric monoxide ( $\bullet NO$ ) with superoxide anion ( $O_2^{\bullet -}$ ). These two radicals forming peroxyxynitrite ( $ONOO^-$ ) which is unstable and will end in the generation of nitrate [43]. With a change in excitation frequency,  $NO_2^-$ ,  $NO_3^-$  (Fig. 4C) and  $H_2O_2$  (Fig. 4D) concentrations can be varied.

A decrease in  $NO_3^-$ ,  $NO_2^-$  and  $H_2O_2$  concentration are clearly visible with an increase in excitation frequency from 11 to 26 kHz for the reason mentioned above. The ability to modify the quantity of reactive species production while keeping the other plasma

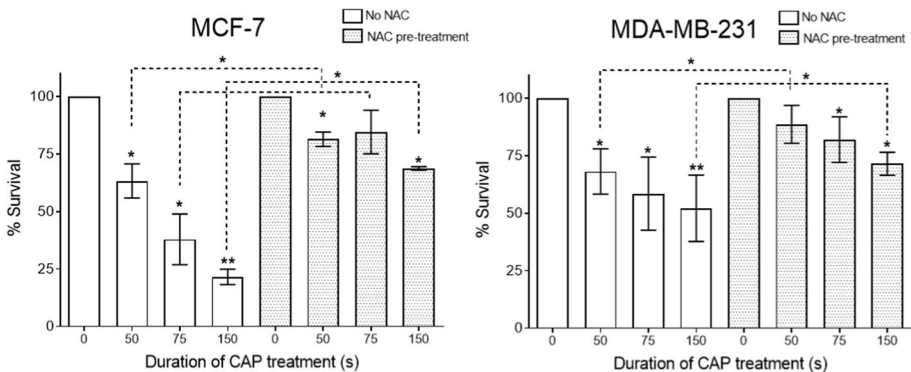


**Fig. 9** CAP induced reduction in proliferation of MCF-7 and MDA-MB-231 breast cancer cell lines is mediated through ROS (Excitation frequency: 11 kHz). MCF-7 cells or MDA-MB-231 cells are treated with 11 kHz frequency CAP for the indicated durations as per the protocol given in Fig. 7A and allowed to grow in the presence and absence of anti-oxidant ROS scavenger NAC. After 48 h, proliferation of cells is analysed. Similarly, the other set is treated with ROS scavenger NAC and proliferation is checked. Quantifications are shown. ( $n=3$  biological replicates with at least 3 technical replicates). ANOVA test was performed and the mean of each group was compared with every other group mean. \* $p < 0.05$  and \*\* $p < 0.01$  compared to respective untreated control group or for the intergroup comparisons

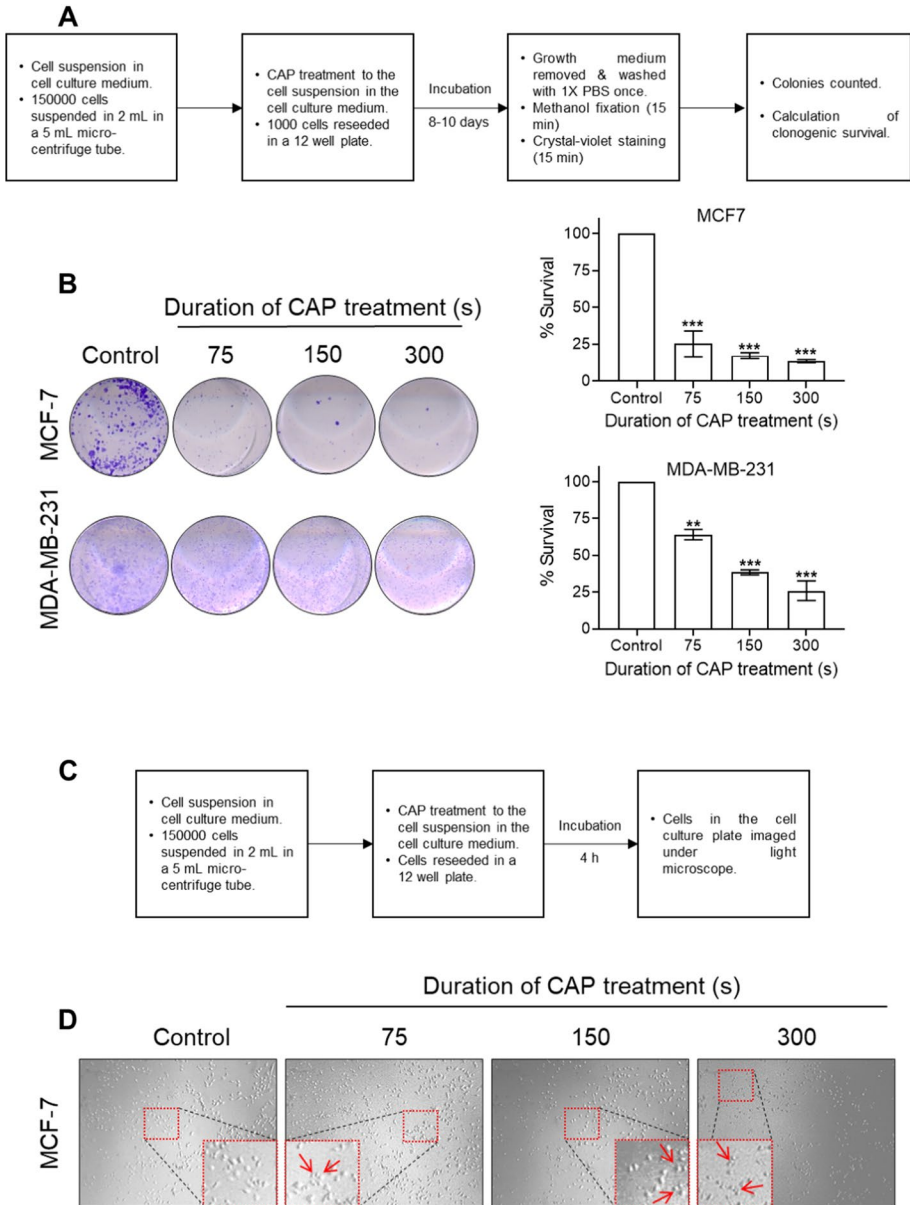
**Fig. 10** CAP treatment reduces cell survival in breast cancer cells (Excitation frequency: 11 kHz). **A** Schematic showing the protocol for treatment of cancer cells with 11 kHz frequency CAP and further analysis. **B** MCF-7 cells or MDA-MB-231 cells are treated with 11 kHz frequency CAP for the indicated durations of time as per the protocol given in A and allowed to grow for 8–10 days to assess the colony forming ability ( $n=3$  biological replicates). Images of the representative wells and quantifications in terms of percentage survival are shown. ANOVA test was performed, and the mean of each group was compared with every other group mean.  $**p < 0.01$  and  $***p < 0.001$  compared to respective untreated control group. **C** Schematic of the protocol used for light microscopy. **D** MCF-7 cells are treated as per the protocol indicated in C for durations mentioned and post 4 h of seeding, observed under a light microscope for morphological changes. Arrows indicate the morphological changes in the treated cells representing damaged or dead cells. **E** Schematic of the protocol used for assessment of apoptotic cells following 11 kHz frequency CAP treatment. **F** MDA-MB-231 cells are treated as per the protocol mentioned in D and apoptotic population is assessed 48 h post treatment by flow cytometry. In the X axis shown in logarithmic scale, the propidium iodide (PI) intensity in arbitrary units (A.U., FL2 channel) is shown which is directly proportional to the DNA content in the cells. The Y axis is the counts (i.e., histogram). **G** MDA-MB-231 cells are treated as per the protocol mentioned in D and cell cycle analysis is performed 24 h post treatment by flow cytometry. In the X axis shown in linear scale, the propidium iodide (PI) intensity in arbitrary units (A.U.) is shown which is directly proportional to the DNA content in the cells. The Y axis is the counts (i.e., histogram). The Sub-G1 cells are omitted from this representation and only cycling cells have been plotted for cell cycle analysis. For F and G, ( $n=3$  biological replicates). ANOVA test was performed and the mean of each group was compared with every other group mean.  $*p < 0.05$ , and  $**p < 0.01$  compared to respective untreated control group

properties constant is substantial in biomedicine since it allows for easy tuning. This modification in  $\text{NO}_3^-$ ,  $\text{NO}_2^-$  and  $\text{H}_2\text{O}_2$  concentration with a change in excitation frequency is also supported by a reduction in pH and an increase in EC.

Figure 5 A, B, C and D present a comparison of the  $\text{H}_2\text{O}_2$ ,  $\text{NO}_3^-$  and  $\text{NO}_2^-$  concentration generated respectively in the plasma treated cell culture medium (DMEM with 10% FBS and  $1 \times$  antibiotic and antimycotic solution) and high purity water for treatment duration of 75 s, 150 s and 300 s respectively. An increase of all the three species with the time of treatment for both media could be observed. It was noticed that the concentration was higher for high purity water as compared to cell culture medium. The effect is due to the presence of foetal bovine serum (FBS) in cell culture media [44]. Most of reactive species react with FBS present in the cell culture media. As a result, the remaining reactive species in media decrease as shown in Fig. 5. Also, cell culture medium is a complex solution consisting of proteins, carbohydrates, amino acids, and lipids and scavenge copious amounts of  $\text{H}_2\text{O}_2$  [45, 46]. Therefore, Fig. 5A shows a larger difference of the  $\text{H}_2\text{O}_2$  generated in both the liquids. The comparable results with different concentration of FBS have been reported by other authors [44–46]. It can be observed that the concentration of species follows the similar trend and increase with increasing time of treatment.

## Optical Emission Spectroscopy

Emission spectroscopy allows for a quick identification of the numerous species present in the plasma jet. The experimental set up is presented in Fig. 6A. Figure 6B shows the cold plasma jet's optical emission spectra (OES) obtained in the wavelength range of 250–900 nm. The intensity variation with the excitation frequency have been studied and published elsewhere [34]. Lower intensity peaks were obtained at higher excitation frequencies as lower ionization and excitation is expected due to lower voltage developed across transformer secondary for plasma generation. The spectrum at an excitation



frequency of 22 kHz reveals the existence of Nitric oxide (NO) and OH bands, along with N<sub>2</sub> bands. There are additional atomic lines that correspond to argon (Ar), atomic oxygen (O), and atomic nitrogen (N). All of these species demonstrate that high energy electrons in plasma can dissociate the ambient air molecules and create reactive oxygen and nitrogen species, which are important for destroying cancer cells. These species can produce long-lived and short-lived species in water, which can affect cell signalling and can also lead to oxidative stress [40]. Hydrogen peroxide (H<sub>2</sub>O<sub>2</sub>) could cause damage to cell walls,

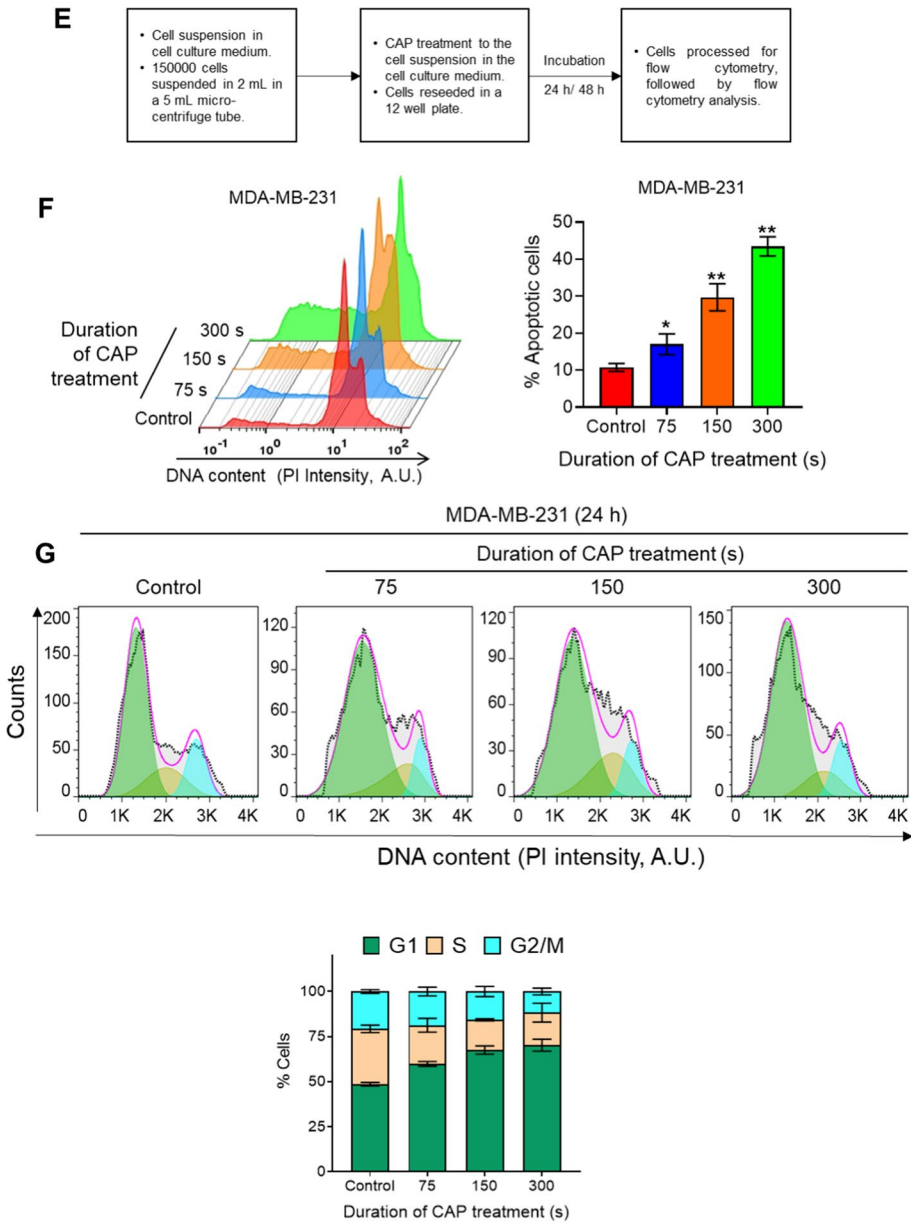


Fig. 10 (continued)

membranes, and intracellular components [40]. Hydroxyl radicals and nitric oxide generated from Plasma treated water has been reported to cause lipid peroxidation, DNA damage, and protein dysfunction [42].



## Biological Studies

### Effect of Excitation Frequency and Treatment Duration on Cell Viability

Ability to divide and proliferate unhindered is a hallmark of cancer cells [47]. A proliferation assay to assess the potential of the CAP treatment to reduce the proliferation of cancer cell was performed. The protocol is as graphically shown in Fig. 7A. Proliferation assay was carried out with all the frequencies and described in the previous section. One frequency, which was highly effective among the tested frequencies, was then selected for further biological experimentation. It was observed that 11 kHz frequency CAP was significantly effective in reducing the cell survival compared to other tested frequencies *i.e.*, 14, 22 and 26 kHz in both the breast cancer cell lines: MCF-7 and MDA-MB-231, when treated for 150 s (Fig. 7B). This data corroborated with the data obtained for the generation of long-lived reactive species discussed in the Fig. 4 and indicated a role for the ROS in cell death induction. Hence, the further biological experiments were carried out only using the 11 kHz frequency CAP treatment.

Further, the effect of 11 kHz frequency CAP treatment for different durations of exposure on the cell survival was assessed (Fig. 8). Survival of both the tested breast cancer cell lines decreased with the increase in the time of exposure to CAP. It was also observed that the effect of CAP was greater in MCF-7 compared to MDA-MB-231 cells. Although a comparison between the two cell lines is drawn here, it is important to note that these two cell lines differ in their genetic constitution [48]. These have inherent genetic differences and also differences in origin. MCF7 is a Luminal A type breast cancer cell line having estrogen receptor (ER), progesterone receptor (PR) and is Her2 positive. MDA-MB-231 is a triple negative breast cancer cell line with no expression of estrogen receptor (ER), progesterone receptor (PR) and is Her2 negative [48]. Sensitivities to anti-cancer agents are governed by a multitude of factors including inherent genetic differences like p53 status, BRCA status and other genetic variables. While the difference in sensitivity to CAP is evident, it is important to note that survival of both the cell lines is significantly hampered.

### Role of ROS in CAP Induced Cell Death

Experiments were also carried out to examine if the effect of CAP on breast cancer cell death is due to the generation of ROS. In this regard, we looked at the effects of 11 kHz frequency CAP treatment in the presence or absence of N-acetyl cysteine (NAC), a well-known antioxidant [49, 50], throughout a range of exposure times. It is found that while the survival of both the breast cancer cell lines decreased with the increase in time of exposure to CAP in the absence of NAC, this was significantly reduced in the presence of NAC (Fig. 9). This clearly suggested a role for ROS in CAP induced cell death. Previous reports have shown that the major mechanism of action of CAP is mediated through the generation of ROS [22, 51].

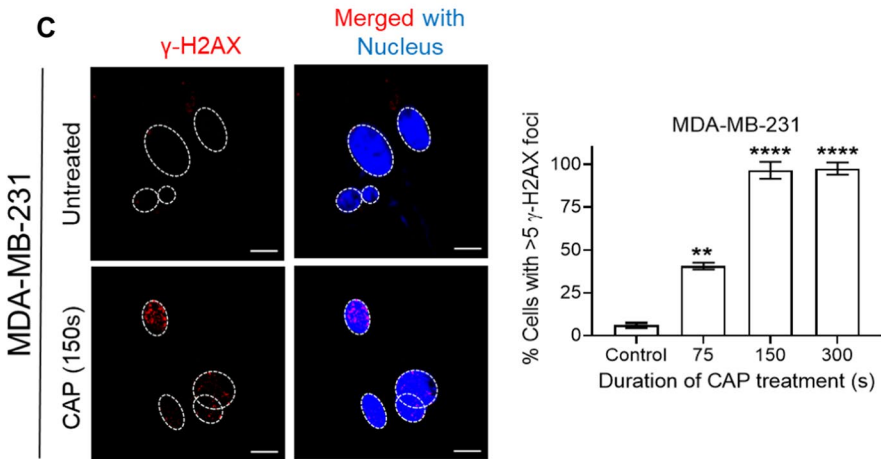
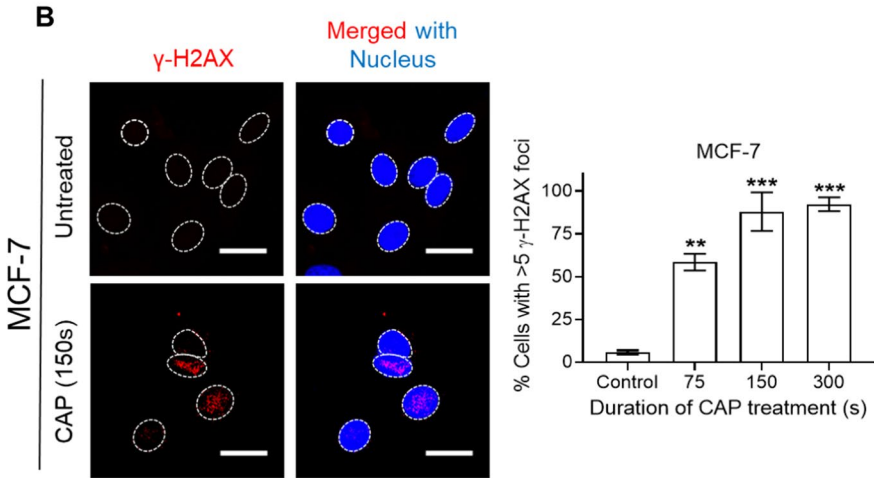
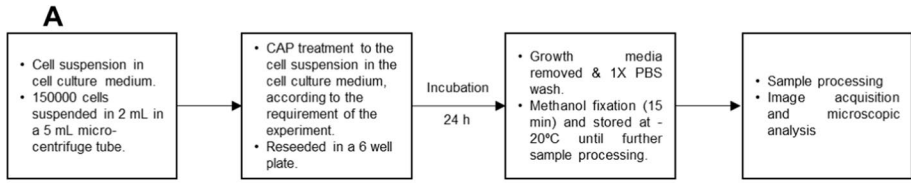
**Fig. 11** CAP treatment induces extensive DNA damage in breast cancer cells (Excitation frequency: 11 kHz). **A** Schematic showing the protocol for treatment of cancer cells with 11 kHz frequency CAP and further analysis for DNA damage analysis by microscopy. **B** MCF-7 cells or **C** MDA-MB-231 cells are treated with 11 kHz frequency CAP for indicated time periods and allowed to attach. 6 h post incubation in a 6-well plate, the cells are fixed and immunofluorescence microscopy is carried out to assess  $\gamma$ -H2AX foci formation. Quantifications are shown. ( $n=3$  biological replicates). ANOVA test was performed and the mean of each group was compared with every other group mean.  $**p<0.01$ ,  $***p<0.001$  and  $****p<0.0001$  compared to respective untreated control group. Scale bar: 20  $\mu\text{m}$ . **D** MCF-7 cells or **E** MDA-MB-231 cells are treated with 11 kHz frequency CAP for 150 s as per the protocol given in **A** and reseeded in a 6-well plate and allowed to attach. 6 h post incubation, the cells are fixed and immunofluorescence microscopy is carried out to assess foci formation. Quantifications are shown. ( $n=3$  biological replicates). ANOVA test was performed and the mean of each group was compared with every other group mean.  $**p<0.01$ ,  $***p<0.001$  and  $****p<0.0001$  compared to respective untreated control group. Scale bar: 20  $\mu\text{m}$

In corroboration with these reports, our data obtained with the plasma treated water and that with NAC treatment indicate that ROS is generated in at 11 kHz frequency and is able to effectively reduce cell proliferation of cancer cells.

### CAP Treatment Reduces Clonogenic Potential with Enhanced Apoptosis and Cell Cycle Arrest in Breast Cancer Cells

In order to understand the cellular mechanism of CAP induced cell death, multiple experiments were carried out. First, the effects of 11 kHz CAP on the clonogenic efficiency of MCF-7 and MDA-MB-231 cells were tested. The protocol for the assay carried has been described in Fig. 10A. It is observed that the clonogenic survival, a measure of the reproductive ability of the cells, of both the MCF-7 and MDA-MB-231 cells were reduced significantly upon CAP treatment (Fig. 10A, B). MCF-7 cells lack caspase-3 and do not efficiently undergo apoptosis [52]. Hence, the effect of CAP on MCF-7 morphology, which can be considered as an indirect measure of cellular health was assessed [53, 54]. We found that the morphology of MCF-7 cells is significantly affected and appeared rounded upon treatment with CAP in an exposure time dependent manner which indicated cell death or cellular damage (Fig. 10C, D). The induction of apoptosis in MDA-MB-231 cells was also assessed. It was observed that the CAP treatment induced apoptosis in MDA-MB-231 cells in a CAP-treatment duration dependent manner (Fig. 10E).

Any dividing cell, cancer cells included, can exist in different phases of the cell cycle viz. Gap 1 (G1), Synthesis (S), Gap 2 (G2)/ Mitosis (M). If there is DNA damage or an event preventing the cell division, the damaged cells tend to accumulate in certain cell cycle phases, allowing repair and recuperation to take place. The accumulation depends on the type of damage and the cell type. If the cells are not able to recover from the damage even after prolonged arrest in the respective cell cycle phases, the cells eventually undergo cell death by apoptosis [55]. Therefore, the effect of CAP on cell cycle in MDA-MB-231 cells was studied, in which the CAP treatment induced a prominent G1-phase cell cycle arrest in MDA-MB-231 cells (Fig. 10F). Further, cell cycle distribution of MDA-MB-231 cells in response to CAP treatments was assessed and has been indicated in the Fig. 10G. Our results showed that CAP treatments induce cell cycle arrest in G1-phase in dose dependent manner.



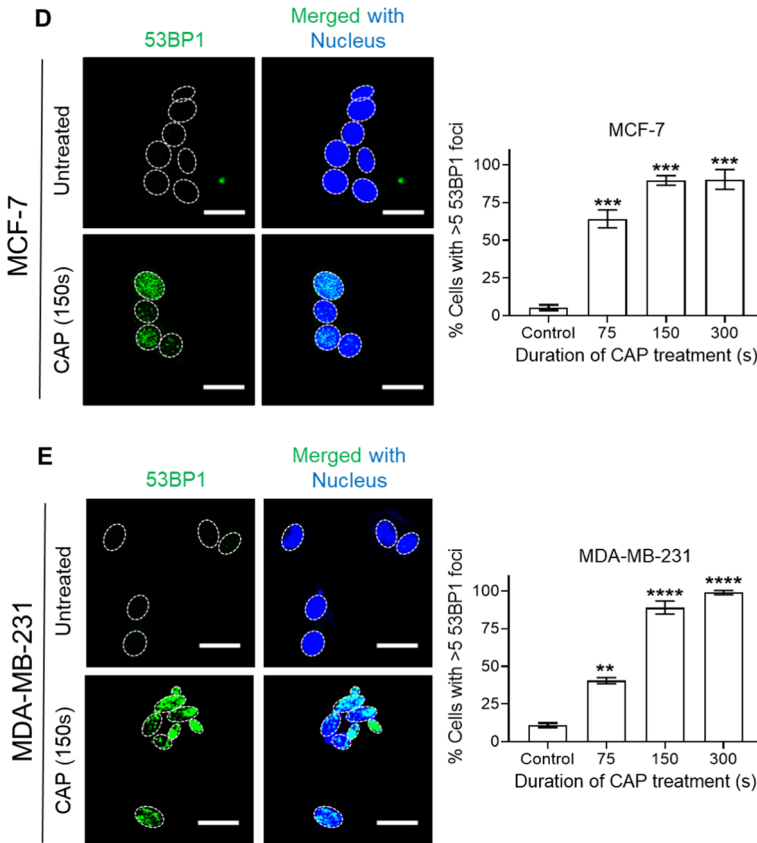


Fig. 11 (continued)

DNA is one of the major targets for the ROS generated by CAP. Faithful repair of DNA damage is essential for the progress of cells from one phase of the cell cycle to the next [56]. In the absence of repair or excessive DNA damage the cells tend to get arrested in the cell cycle and prolonged arrest eventually leads to apoptosis [56]. We observed prominent G1 phase arrest in the cell cycle indicative of DNA damage due to the production of ROS by CAP treatment.

### CAP Treatment Induces DNA Damage in Breast Cancer Cells

Cell cycle arrest in G1 phase was indicative of DNA damage due to CAP treatment. To test whether DNA damage is induced in cancer cells, a microscopic analysis of DNA double strand break (DSB) marker proteins,  $\gamma$ -H2AX and 53BP1 by immunostaining is performed [57, 58]. Phosphorylation of H2AX variant of H2A histone on Ser 139 i.e.,  $\gamma$ -H2AX is one of the characteristic and important post-translational modification and the basis for signalling of the DNA damage in cells. The levels of this phosphorylated variant of H2AX protein are upregulated upon DNA damage and hence can be used as a surrogate marker to understand the extent of DNA damage in cells. Consequent to the formation of DNA

double strand breaks in cells, p53 Binding protein (53BP1) is one of the first responders to the DNA ends and hence is considered a marker for DNA DSBs [57, 58]. In our work, we have immunostained for the detection of these two proteins by using immunofluorescence microscopy using the protocol mentioned in (Fig. 11A).

It was observed that percentage of cells with DNA DSBs, as assessed by  $\gamma$ -H2AX and 53BP1 positive nuclei, were increased significantly with increasing duration of CAP treatment. It is evident from the Fig. 11B, C for  $\gamma$ -H2AX staining in MCF-7 and MDA-MB-231 respectively. And similarly, Fig. 11D, E for 53BP1 staining in MCF-7 and MDA-MB-231 respectively. This indicated that the 11 kHz frequency CAP treatment induces DNA DSBs in breast cancer cells.

Taken together, the data we have presented here indicate that among the frequencies generated by the reported EFCAP device and tested in this study, 11 kHz CAP treatment is the most efficacious in reducing the proliferation of breast cancer cells. 11 kHz frequency CAP induces reactive oxygen species mediated DNA damage leading to cell cycle arrest and eventually apoptosis in breast cancer cells.

## Conclusions

Cold atmospheric plasma treatment has presented itself as a novel modality of therapy for a multitude of cancer types. In this regard, to the best of our knowledge, this work is the first to assess the effects of excitation frequency controlled cold atmospheric pressure plasma (EFCAP) on breast cancer cells. The non-dielectric cold plasma source could tune the amount of long-lived ROS generated in plasma treated water by changing the excitation frequency. The presence of oxygen and nitrogen species were distinctly seen in the OES spectrum of the plasma jet. These species might serve as the precursor for the generation of long-lived reactive species in the medium. When the frequency is low, a larger voltage is created at the secondary of the transformer, which results in better ionization in the plasma jet. The discharge zone obtained for various frequencies appears to follow diverse patterns and clearly demonstrates a shift of the discharge dynamics with the change in excitation frequency. Water is treated to determine the influence of change in frequency of excitation on plasma water interaction. The electrical conductivity (EC), concentrations of  $\text{NO}_3^-$ ,  $\text{NO}_2^-$  and  $\text{H}_2\text{O}_2$  increased with treatment time, but the pH was found to decrease. The expected variation in the concentration of these species with a change in frequency of excitation is clearly noticeable. A higher EC and a higher concentration of long-lived reactive species at different frequencies clearly demonstrate the potential of the device.

In this work, we first standardized the distance for the treatment with cold-atmospheric plasma to the attached and suspension cell culture models and decided to study the effects at 15 mm from the CAP nozzle exit to the well/tube top in inducing cell death in the tested breast cancer cell lines. Further, the proliferation assay was carried out at four different excitation frequencies viz. 11, 14, 22, and 26 kHz. Among the frequencies tested, we also observed that the 11 kHz frequency is the most efficient in reducing breast cancer cell proliferation. This corroborated with the potential of the 11 kHz frequency to produce higher amounts of reactive species as discussed in the results. The effect of CAP treatment varied with used excitation frequency of the CAP and duration of the CAP treatment.

The optimized parameters of the device were demonstrated for the induction of breast cancer cell death. Excitation at 11 kHz frequency is found to cause more cell death than 14 kHz, 22 kHz, and 26 kHz excitation. Ease of generating variable concentration of

reactive species like  $\text{NO}_3^-$ ,  $\text{NO}_2^-$  and  $\text{H}_2\text{O}_2$  simply by changing excitation frequency is a novel aspect of the device. Further studies are required to custom induce reactive species in the medium to study their effect in inducing cancer cell death.

**Supplementary Information** The online version contains supplementary material available at <https://doi.org/10.1007/s11090-023-10312-3>

**Acknowledgements** Authors wish to acknowledge valuable helps received from Mr Tushar Hire (L&PTD, BARC) during EFCAP operation. Authors thank Head, L&PTD, GD, BTDG and GD, BSG for their kind support.

## References

1. Penkov OV, Khadem M, Lim WS, Kim DE (2015) A review of recent applications of atmospheric pressure plasma jets for materials processing. *J Coat Technol Res* 12:225–235
2. Domonkos M, Demo P, Kromka A (2020) Nanosphere lithography for structuring polycrystalline diamond films. *Crystals* 10:118
3. Li YF, Shimizu T, Zimmermann JL, Morfill GE (2012) Cold atmospheric plasma for surface disinfection. *Plasma Process Polym* 9:585
4. Laroussi M, LuX KeidarM (2017) Perspective: the physics, diagnostics, and applications of atmospheric pressure low temperature plasma sources used in plasma medicine. *J Appl Phys* 122:020901
5. Fridman G, Friedman G, Gutsol A, Shekhter AB, Vasilets VN, Fridman A (2008) Applied Plasma Medicine. *Plasma Process Polym* 5:503
6. Attri P, Yusupov M, Park JH, Lingamdinne LP, Koduru JR, Shiratani M, Choi EH, Bogaerts, (2016) A Mechanism and comparison of needle-type non-thermal direct and indirect atmospheric pressure plasma jets on the degradation of dyes. *Sci Rep* 6:34419
7. Smet C, Baka M, Dickenson A, Walsh JL, Valdramidis VP, Impe JFP (2017) Antimicrobial efficacy of cold atmospheric plasma for different intrinsic and extrinsic parameters. *Plasma Process Polym* 15:1700048
8. Kamionka J, Matthes R, Holtfreter B, Pink C, Schlüter R, Woedtke T, Kocher T, Jablonowski L (2022) Efficiency of cold atmospheric plasma, cleaning powders and their combination for biofilm removal on two different titanium implant surfaces. *Clin Oral Investig* 26(3):3179–3187
9. Xiang L, Xu X, Zhang S, Caia D, Dai X (2018) Cold atmospheric plasma conveys selectivity on triple negative breast cancer cells both in vitro and in vivo. *Free Radical Biol Med* 124:205–213
10. Keidar M (2015) Plasma for cancer treatment. *Plasma Sources Sci Technol* 24:033001
11. Winter J, Brandenburg R, Weltmann KD (2015) Atmospheric pressure plasma jets: an overview of devices and new directions. *Plasma Sources Sci Technol* 24:064001
12. Hoffmann C, Berganza C, Zhang J (2013) Cold Atmospheric Plasma: methods of production and application in dentistry and oncology. *Med Gas Res* 3:21
13. Bauer G, Sersenova D, Graves DB, Machala Z (2019) Cold Atmospheric plasma and plasma-Activated Medium trigger RONS-Based tumor cell Apoptosis. *Sci Rep* 9:14210
14. Mahdikia H, Shokri B, Majidzadeh AK (2021) The feasibility study of plasma-activated water as a physical therapy to induce apoptosis in melanoma cancer cells in-vitro. *Iran J Pharm Res* 20(3):337–350
15. Sersenová D, Machala Z, Repiská V, Gbelcová H (2021) Selective apoptotic effect of plasma activated liquids on human cancer cell lines. *Molecules* 26(14):4254
16. Cancer (2021) <https://www.who.int/news-room/fact-sheets/detail/cancer> (accessed October 2021)
17. Ferlay J, Ervik M, Lam F, Colombet M, Mery L, Piñeros M (2020) Global Cancer Observatory: Cancer Today. Lyon: International Agency for Research on Cancer; (<https://gco.iarc.fr/today>, accessed February 2021).
18. IARC (2021) Cancer fact sheets, <https://gco.iarc.fr/today/data/factsheets/cancers/39-All-cancers-fact-sheet.pdf> (accessed October 2021)
19. Carelle N, Piotto E, Bellanger A, Germanaud J, Thuillier A, Khayat D (2002) Changing patient perceptions of the side effects of cancer chemotherapy. *Cancer* 95(1):155–163
20. Mansoori B, Mohammadi A, Davudian S, Shirjang S, Behzad B (2017) The different mechanisms of cancer drug resistance: a brief review. *Adv Pharm Bull* 7(3):339–348

21. Longley DB, Johnston PG (2005) Molecular mechanisms of drug resistance. *J Pathol* 205(2):275–292
22. Yan D, Sherman JH, Keidar M (2017) Cold atmospheric plasma, a novel promising anti-cancer treatment modality. *Oncotarget* 8(9):15977–15995
23. Koritzer J, Boxhammer V, Schafer A, Shimizu T, Klampfl TG, Li YF, Welz C, Schwenk-Zieger S, Morfill GE, Zimmermann JL, Schlegel J (2013) Restoration of sensitivity in chemo-resistant glioma cells by cold atmospheric plasma. *PLoS ONE* 8(5):e64498
24. Ishaq M, Han ZJ, Kumar S, Evans MD, Ostrikov KK (2015) Atmospheric-pressure plasma-and TRAIL-induced apoptosis in TRAIL-resistant colorectal cancer cells. *Plasma Processes Polym* 12(6):574–582
25. Wang M, Holmes B, Cheng X, Zhu W, Keidar M, Zhang LG (2013) Cold atmospheric plasma for selectively ablating metastatic breast cancer cells. *PLoS ONE* 8(9):e73741
26. Preston RG, Ogawa T, Uemura M, Shumulinsky G, Valle BL, Pirini F (2014) Cold atmospheric plasma treatment selectively targets head and neck squamous cell carcinoma cells. *Int J Mol Med* 34(4):941–946
27. Saadati F, Mahdikia H, Abbaszadeh HA, Abdollahifar MA, Khoramgah MS, Shokri B (2018) Comparison of Direct and Indirect cold atmospheric-pressure plasma methods in the B<sub>16</sub>F<sub>10</sub> melanoma cancer cells treatment. *Sci Rep* 8(1):7689
28. Akishev YS, Balakirev AA, Grushin ME, Karalnik VB, Medvedev MA, Petryakov AV, TNI (2020) Pin-to-plane self-pulsing discharge in transversal airflow: interaction with a substrate of plasma filaments blown out from the discharge zone. *Plasma Sources Sci Technol* 29:045012
29. Fridman G, Peddinghaus M, Ayan H, Fridman A, Balasubramanian M, Gutsol A, Brooks A, Friedman G (2006) Blood coagulation and living tissue sterilization by floating-electrode dielectric barrier discharge in air. *Plasma Chem Plasma Process* 26:425–442
30. Stoffels E, Flikweert AJ, Stoffels WW, Kroesen GMW (2002) Plasma needle: a non-destructive atmospheric plasma source for fine surface treatment of (bio)materials. *Plasma Sources Sci Technol* 11:383–388
31. Park J, Henins I, Herrmann HW, Selwyn GS, Jeong JY, Hicks RF, Shim D, Chang CS (2000) An atmospheric pressure plasma source. *Appl Phys Lett* 76(3):288–290
32. Tiwari N, Misra VC, Ghorui S (2022) Study of unique aspects of oxidative-nitrosative environment in a radio frequency cold plasma device. *Vacuum* 205:111407
33. Ghorui S (2022) A novel excitation frequency controlled cold atmospheric pressure plasma device and its unique discharge behaviour. *Pramana J Phys* 96:147
34. Misra VC, Tiwari N, Ghorui S (2022) Characterization and investigation of the unique plasma behavior caused by variable driving frequencies in the formation of cold atmospheric plasma. *Curr Appl Phys* 41:92–99
35. Bellare GP, Patro BS (2022) Resveratrol sensitizes breast cancer to PARP inhibitor, talazoparib through dual inhibition of AKT and autophagy flux. *Biochem Pharma* 199:115024
36. Bellare GP, Saha B, Patro BS (2021) Targeting autophagy reverses de novo resistance in homologous recombination repair proficient breast cancers to PARP inhibition. *Br J Cancer* 124:1260–1274
37. Nie D, Wang W, Yang D, Shi H, Huo Y, Dai L (2011) Optical study of diffuse bi-directional nanosecond pulsed dielectric barrier discharge in nitrogen. *Spectrochim. Acta Part A* 79:1896–1903
38. Elsayah M, Ghafar HHA, Morgan NN, Hassaballa S, Samir A, Elakshar FF, Garamoon AA (2012) Corona discharge with electro-spraying system for phenol removal from water. *IEEE Trans Plasma Sci* 40:29–33
39. Parvulescu VI, Magureanu M, Lukes P (2012) *Plasma Chemistry and Catalysis in Gases and Liquids*, Wiley, Hoboken, NJ
40. Hu X, Zhang Y, Wu RA, Liao X, Liu D, Cullen PJ, Zhou RW, Ding T (2022) Diagnostic analysis of reactive species in plasma-activated water (PAW): current advances and outlooks. *J Phys D Appl Phys* 55:023002
41. Svarnas P, Poupouzas M, Papalexopoulou K, Kalaitzopoulou E, Skipitari M, Papadea P, Varmenou A, Giannakopoulos E, Georgiou CD, Georga S, Krontiras C (2022) Water modification by cold plasma jet with respect to physical and chemical properties. *Appl Sci* 12:11950
42. Xiang QS, Zhang R, Fan LM, Ma YF, Wu D, Li K, Bai YF (2020) Microbial inactivation and quality of grapes treated by plasma-activated water combined with mild heat LWT-Food Sci. Technol 126:109336
43. Radi R (2018) Oxygen radicals, nitric oxide, and peroxy nitrite: Redox pathways in molecular medicine. *PNAS* 115(23):5839–5848
44. Yan D, Jonathan HS, Xiaoqian C, Ratovitski E, Canady J, Keidar M (2014) Controlling plasma stimulated media in cancer treatment application. *Appl Phys Lett* 105:224101

45. Tresp H, Malte UH, Weltmann KD, Reuter S (2013) Effects of atmosphere composition and liquid type on plasma-generated reactive species in biologically relevant solutions. *Plasma Med* 3(1–2):45–55
46. Boehm D, Heslin C, Cullen PJ, Bourke P (2016) Cytotoxic and mutagenic potential of solutions exposed to cold atmospheric plasma. *Sci Rep* 6:21464
47. Hanahan D, Weinberg RA (2011) Hallmarks of cancer: the next generation. *Cell* 144:646–674
48. Dai X, Cheng H, Bai Z, Li J (2017) Breast cancer cell line classification and its relevance with breast tumor subtyping. *J Cancer* 8(16):3131–3141
49. Lee S, Lee H, Jeong D, Ham J, Park S, Choi EH, Kim SJ (2017) Cold atmospheric plasma restores tamoxifen sensitivity in resistant MCF-7 breast cancer cell. *Free Radic Biol Med* 110:280–290
50. Zhitkovich A (2019) N-acetylcysteine: antioxidant, aldehyde scavenger, and more. *Chem Res Toxicol* 32:1318–1319
51. Yan D, Talbot A, Nourmohammadi N, Cheng X, Canady J, Sherman J, Keidar M (2015) Principles of using cold atmospheric plasma stimulated media for cancer treatment. *Sci Rep* 5:18339
52. Yang XH, Sladek TL, Liu X, Butler BR, Froelich CJ, Thor AD (2001) Reconstitution of caspase 3 sensitizes MCF-7 breast cancer cells to doxorubicin- and etoposide-induced apoptosis. *Cancer Res* 61:348–354
53. Häcker G (2000) The morphology of apoptosis. *Cell Tissue Res* 301:5–17
54. Murad H, Hawat M, Ekhtiar A, AlJapawe A, Abbas A, Darwish H, Sbenati O, Ghannam A (2016) Induction of G1-phase cell cycle arrest and apoptosis pathway in MDA-MB-231 human breast cancer cells by sulfated polysaccharide extracted from *Laurencia papillosa*. *Cancer Cell Int* 16:39
55. Chen J (2016) The cell-cycle arrest and apoptotic functions of p53 in tumor initiation and progression. *Cold Spring Harb Perspect Med* 6(3):a026104
56. Hustedt N, Durocher D (2017) The control of DNA repair by the cell cycle. *Nat Cell Biol* 19:1–9
57. Mah LJ, Osta AE, Karagiannis TC (2010) gammaH<sub>2</sub>AX: a sensitive molecular marker of DNA damage and repair. *Leukemia* 24:679–686
58. Panier S, Boulton SJ (2014) Double-strand break repair: 53BP1 comes into focus. *Nat Rev Mol Cell Biol* 15:7–18

**Publisher's Note** Springer Nature remains neutral with regard to jurisdictional claims in published maps and institutional affiliations.

Springer Nature or its licensor (e.g. a society or other partner) holds exclusive rights to this article under a publishing agreement with the author(s) or other rightsholder(s); author self-archiving of the accepted manuscript version of this article is solely governed by the terms of such publishing agreement and applicable law.